Experimental and Computational Study of Steric and Electronic Effects on the Coordination of Bulky, Water-Soluble Alkylphosphines to Palladium under Reducing Conditions: Correlation to Catalytic Activity

Rebecca B. DeVasher, Jason M. Spruell, David A. Dixon, Grant A. Broker, Scott T. Griffin, Robin D. Rogers, and Kevin H. Shaughnessy*

Department of Chemistry and Center for Green Manufacturing, The University of Alabama, Box 870336, Tuscaloosa, Alabama 35487-0336

Received October 1, 2004

Sterically demanding, water-soluble alkylphosphine ligands 2-(di-*tert*-butylphosphino)-ethyltrimethylammonium chloride (*t*-Bu-Amphos) and 4-(di-*tert*-butylphosphino)-*N,N*-dimethylpiperidinium chloride (*t*-Bu-Pip-phos) in combination with palladium salts provided active catalysts for the cross-coupling of aryl halides under mild conditions in aqueous solvents, whereas 4-(dicyclohexylphosphino)-*N,N*-dimethylpiperidinium chloride (Cy-Pip-phos) gave a less active catalyst. Catalyst activity increased with increasing cone angle of the ligands, but the χ electronic parameter determined from the symmetric C−O stretching frequency of $LNi(CO)_3$ did not correlate with catalyst activity. Catalyst activity correlated with other calculated electronic parameters, such as the HOMO−LUMO energy gap of the ligand and the HOMO energy level of the LPd(0) species. Multinuclear NMR spectroscopic studies showed that *t*-Bu-Amphos and *t*-Bu-Pip-phos rapidly form $L_2Pd(0)$ (L = *t*-Bu-Amphos or *t*-Bu-Pip-phos) complexes when reacted with $Pd(OAc)_2$ under reducing conditions over a range of L:Pd ratios. In contrast, the coordination chemistry of Cy-Pip-phos depended on the Cy-Pip-phos:Pd ratio. At a ≤1:1 Cy-Pip-phos:Pd ratio, rapid formation of $L_2Pd(0)$ occurred. At higher L:Pd ratios, initial formation of *trans*-$(Cy\text{-}Pip\text{-}phos)_2PdCl_2$ was observed followed by slow reduction to the Pd(0) complex.

Introduction

Palladium-catalyzed cross-coupling reactions, such as the Heck,[1,2] Suzuki,[3−5] Sonogashira,[6] and Hartwig−Buchwald couplings,[7−10] have become widely used methods for formation of C−C and C−heteroatom bonds. Although some of these reactions have been known for over thirty years, there is still significant interest in developing catalyst systems that provide more active and stable catalysts. Triphenylphosphine, and related arylphosphines, remain popular ligand choices, but catalysts derived from arylphosphines suffer from modest activity, particularly toward less reactive aryl halides, and undesirable side reactions. Recent research has shown that alternative ligands such as sterically demanding trialkylphosphines,[9−22] *N*-heterocyclic carbenes,[23−27] and ligands capable of forming palladacycles[28] give catalyst that are highly active, even toward aryl chloride substrates, under mild temperatures.

The high activity of catalysts derived from alkylphosphines or *N*-heterocyclic carbenes is believed to depend on both the steric demand and electron-donating ability of these ligands. The steric bulk of the ligand promotes formation of coordinatively unsaturated LPd(0) (L = phosphine, *N*-heterocyclic carbene) active species (Scheme 1). Although the proposed "LPd(0)" complex shown in

* To whom correspondence should be addressed. E-mail: kshaughn@bama.ua.edu.

(1) Beletskaya, I. P.; Cheprakov, A. V. *Chem. Rev.* **2000**, *100*, 3009−3066.
(2) Whitcombe, N. J.; Hii, K. K.; Gibson, S. E. *Tetrahedron* **2001**, *57*, 7449−7476.
(3) Miyaura, N.; Suzuki, A. *Chem. Rev.* **1995**, *95*, 2457−2483.
(4) Suzuki, A. *J. Organomet. Chem.* **1999**, *576*, 147−168.
(5) Kotha, S.; Lahiri, K.; Kashinath, D. *Tetrahedron* **2002**, *58*, 9633−9695.
(6) Negishi, E.-i.; Anastasia, L. *Chem. Rev.* **2003**, *103*, 1979−2017.
(7) Hartwig, J. F. *Angew. Chem., Int. Ed.* **1998**, *37*, 2046−2067.
(8) Hartwig, J. F. *Acc. Chem. Res.* **1998**, *31*, 852−860.
(9) Wolfe, J. P.; Wagaw, S.; Marcoux, J.-F.; Buchwald, S. L. *Acc. Chem. Res.* **1998**, *31*, 805−818.
(10) Yang, B. H.; Buchwald, S. L. *J. Organomet. Chem.* **1999**, *576*, 125−146.
(11) Wolfe, J. P.; Singer, R. A.; Yang, B. H.; Buchwald, S. L. *J. Am. Chem. Soc.* **1999**, *121*, 9550−9561.
(12) Aranyos, A.; Old, D. W.; Kiyomori, A.; Wolfe, J. P.; Sadighi, J. P.; Buchwald, S. L. *J. Am. Chem. Soc.* **1999**, *121*, 4369−4378.
(13) Hartwig, J. F.; Kawatsura, M.; Hauck, S. I.; Shaughnessy, K. H.; Alcazar-Roman, L. M. *J. Org. Chem.* **1999**, *64*, 5575−5580.
(14) Hundertmark, T.; Littke, A. F.; Buchwald, S. L.; Fu, G. C. *Org. Lett.* **2000**, *2*, 1729−1731.
(15) Kirchhoff, J. H.; Dai, C.; Fu, G. C. *Angew. Chem., Int. Ed.* **2002**, *41*, 1945−1947.
(16) Littke, A. F.; Fu, G. C. *Angew. Chem., Int. Ed.* **2002**, *41*, 4176−4211.
(17) Littke, A. F.; Fu, G. C. *J. Am. Chem. Soc.* **2001**, *123*, 6989−7000.
(18) Littke, A. F.; Dai, C.; Fu, G. C. *J. Am. Chem. Soc.* **2000**, *122*, 4020−4028.
(19) Stambuli, J. P.; Stauffer, S. R.; Shaughnessy, K. H.; Hartwig, J. F. *J. Am. Chem. Soc.* **2001**, *123*, 2677−2678.
(20) Stauffer, S. R.; Beare, N. A.; Stambuli, J. P.; Hartwig, J. F. *J. Am. Chem. Soc.* **2001**, *123*, 4641−4642.
(21) You, J.; Verkade, J. G. *J. Org. Chem.* **2003**, *68*, 8003−8007.
(22) Zapf, A.; Ehrentraut, A.; Beller, M. *Angew. Chem., Int. Ed.* **2000**, *39*, 4153−4155.

10.1021/om049241w CCC: $30.25
Publication on Web 02/04/2005

Scheme 1. General Mechanism for Palladium-Catalyzed Cross-Coupling Reactions with Sterically Demanding Ligands

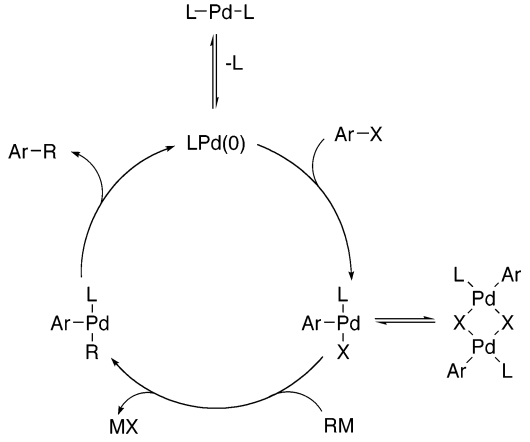

Scheme 1 has not been observed under catalytic conditions, its key role has been inferred from the inverse dependence of catalyst activity on L:Pd ratio,[12,13,18,29] studies of reductive elimination of aryl halides upon complexation of bulky alkylphosphines,[30,31] observation of monophosphine complexes stabilized by other ligands,[29,32,33] and the formation of stable three-coordinate LPd(Ar)X species upon oxidative addition of aryl bromides to a 1:1 mixture of bulky phosphine and Pd(dba)$_2$.[29,34,35] Electron-rich ligands promote oxidative addition, particularly of less reactive aryl halide substrates, by increasing the electron density of the palladium(0) species.

There has been a long-standing interest in aqueous-phase, palladium-catalyzed cross-coupling reactions.[36,37] Water is an attractive replacement for organic solvents because it is inexpensive, renewable, nontoxic, and nonflammable. In addition, the use of water-soluble catalysts in aqueous-biphasic mixtures allows easy separation of the organic product from the catalyst. The most commonly used water-soluble phosphine is TPPTS

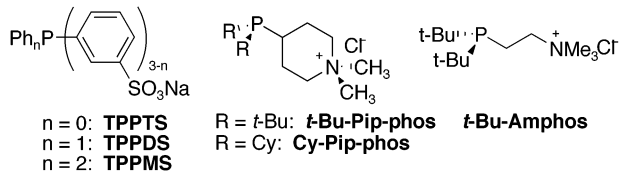

Figure 1. Water-soluble phosphine ligands.

(Figure 1). Since Casalnuovo's original report of Pd-catalyzed cross-coupling reactions using TPPMS (Figure 1),[38] TPPTS and a number of related hydrophilic triarylphosphines have been applied to cross-coupling reactions.[39–46]

Although catalysts derived from these ligands give synthetically useful activities, they often have limited reactivity toward unactivated aryl bromides or aryl chlorides except at high temperatures. Increased electron-donating ability and steric demand are key parameters in designing ligands for palladium-catalyzed coupling reactions of less active substrates, yet there are few examples of sterically demanding, water-soluble alkylphosphine ligands.[47–50] We have shown that sterically demanding, water-soluble trialkylphosphines, such as *t*-Bu-Amphos and *t*-Bu-Pip-phos (Figure 1), provide highly active catalysts for Pd-catalyzed cross-coupling reactions in aqueous solvents.[51,52] Herein, we report the steric and electronic parameters of these ligands and their coordination chemistry with Pd(II) sources under reducing conditions. The cone angles have been calculated based on optimized geometries of Pd–ligand complexes obtained from density functional theory. On the basis of these results, there is a distinct correlation between cone angle and both the activity of catalysts derived from these ligands and their coordination chemistry.

Results

Ligand Synthesis and Structural Characterization. The synthesis of Cy-Pip-phos has been previously reported.[50] The *t*-Bu-Amphos and *t*-Bu-Pip-phos ligands were prepared by a modification of this procedure (Scheme 2).[51] An intermediate in the synthesis of *t*-Bu-Pip-phos, the borane adduct of 4-(di-*tert*-butylphosphino)-*N,N*-piperidinium iodide [*t*-Bu-Pip-phos·BH$_3$]I,

(23) Stauffer, S. R.; Lee, S.; Stambuli, J. P.; Hauck, S. I.; Hartwig, J. F. *Org. Lett.* **2000**, *2*, 1423–1426.
(24) Gstöttmayr, C. W. K.; Böhm, V. P. W.; Herdtweck, E.; Drosche, M.; Herrmann, W. A. *Angew. Chem., Int. Ed.* **2002**, *41*, 1363–1365.
(25) Jørgensen, M.; Lee, S.; Liu, X.; Wolkowski, J. P.; Hartwig, J. F. *J. Am. Chem. Soc.* **2002**, *124*, 12557–12565.
(26) Selvakumar, K.; Zapf, A.; Beller, M. *Org. Lett.* **2002**, *4*, 3031–3033.
(27) Navarro, O.; Kaur, N.; Mahjoor, P.; Nolan, S. P. *J. Org. Chem.* **2004**, *69*, 3173–3180.
(28) Bedford, R. B.; Hazelwood, S. L.; Limmert, M. E.; Albisson, D. A.; Draper, S. M.; Scully, P. N.; Coles, S. J.; Hursthouse, M. B. *Chem. Eur. J.* **2003**, *9*, 3216–3227.
(29) Bei, X.; Turner, H. W.; Weinberg, W. H.; Guram, A. S. *J. Org. Chem.* **1999**, *64*, 6797–6803.
(30) Roy, A. H.; Hartwig, J. F. *J. Am. Chem. Soc.* **2001**, *123*, 1232–1233.
(31) Roy, A. H.; Hartwig, J. F. *Organometallics* **2004**, *23*, 1533–1541.
(32) Andreu, M. G.; Zapf, A.; Beller, M. *Chem. Commun.* **2000**, 2475–2476.
(33) Yin, J.; Rainka, M. P.; Zhang, X.-X.; Buchwald, S. L. *J. Am. Chem. Soc.* **2002**, *124*, 1162–1163.
(34) Stambuli, J. P.; Bühl, M.; Hartwig, J. F. *J. Am. Chem. Soc.* **2002**, *124*, 9346–9347.
(35) Stambuli, J. P.; Incarvito, C. D.; Bühl, M.; Hartwig, J. F. *J. Am. Chem. Soc.* **2004**, *126*, 1184–1194.
(36) Genêt, J. P.; Savignac, M. *J. Organomet. Chem.* **1999**, *576*, 305–317.
(37) Beletskaya, I. P.; Cheprakov, A. V. In *Handbook of Organopalladium Chemistry for Organic Synthesis*; Negishi, E.-i., Ed., John Wiley & Sons: New York, 2002; Vol. 2, pp 2957–3006.
(38) Casalnuovo, A. L.; Calabrese, J. C. *J. Am. Chem. Soc.* **1990**, *112*, 4324–4330.
(39) Genêt, J. P.; Blart, E.; Savignac, M. *Synlett* **1992**, 715–717.
(40) Genêt, J. P.; Linquist, A.; Blard, E.; Mouries, V.; Savignac, M.; Vaultier, M. *Tetrahedron Lett.* **1995**, *36*, 1443–1446.
(41) Amatore, C.; Blart, E.; Genêt, J. P.; Jutand, A.; Lemaire-Audoire, S.; Savignac, M. *J. Org. Chem.* **1995**, *60*, 6829–6839.
(42) Paetzold, E.; Oehme, G. *J. Mol. Catal. A: Chem.* **2000**, *152*, 69–76.
(43) Beller, M.; Krauter, J. G. E.; Zapf, A. *Angew. Chem., Int. Ed. Engl.* **1997**, *36*, 772–774.
(44) Hessler, A.; Stelzer, O.; Dibowski, H.; Worm, K.; Schmidtchen, F. P. *J. Org. Chem.* **1997**, *62*, 2362–2369.
(45) Villemin, D.; Nechab, B. *J. Chem. Res., Synop.* **2000**, 429–431.
(46) Kolodziuk, R.; Penciu, A.; Tollabi, M.; Framery, E.; Goux-Henry, C.; Iourtchenko, A.; Sinou, D. *J. Organomet. Chem.* **2003**, *687*, 384–391.
(47) Wolf, C.; Lerebours, R. *J. Org. Chem.* **2003**, *68*, 7551–7554.
(48) Wolf, C.; Lerebours, R. *Org. Lett.* **2004**, *6*, 1147–1150.
(49) Nishimura, M.; Ueda, M.; Miyaura, N. *Tetrahedron* **2002**, *58*, 5779–5787.
(50) Mohr, B.; Lynn, D. M.; Grubbs, R. H. *Organometallics* **1996**, *15*, 4317–4325.
(51) Shaughnessy, K. H.; Booth, R. S. *Org. Lett.* **2001**, *3*, 2757–2759.
(52) DeVasher, R. B.; Moore, L. R.; Shaughnessy, K. H. *J. Org. Chem.* **2004**, *69*, 7919–7927.

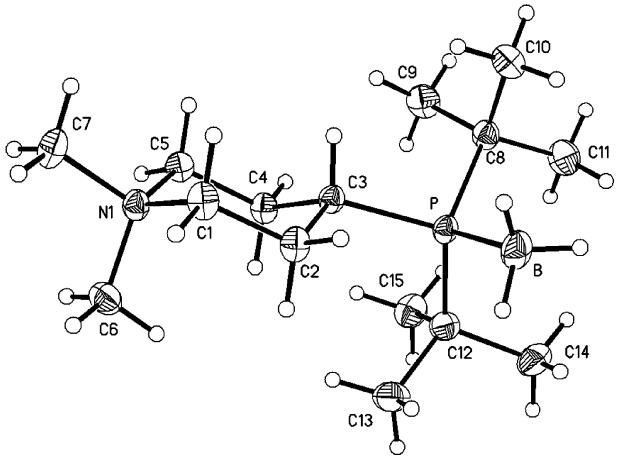

Figure 2. ORTEP diagram of [*t*-Bu-Pip-phos·BH_3]I. The iodide anion has been omitted. Ellipsoids are drawn at the 50% probability level. Hydrogen atoms were placed in idealized positions.

Table 1. Selected Bond Lengths and Angles for [*t*-Bu-Pip-phos·BH_3]I and Calculated (DFT-LDA) Values for *t*-Bu-Pip-phos

bond length	X-ray (Å)	calcd[a] (Å)	bond angle	X-ray (deg)	calc[a] (deg)
P−C3	1.857(2)	1.899	C3−P−C12	110.17(10)	110.2
P−C8	1.880(2)	1.892	C3−P−C8	104.38(9)	98.6
P−C12	1.876(2)	1.893	C12−P−C8	112.96(10)	111.2
P−B	1.934(2)		C2−C3−P	112.75(14)	106.3
			C4−C3−P	119.40(14)	120.8

[a] Calculated geometry (DFT, local density approximation (LDA)) of the free *t*-Bu-Pip-phos ligand.

was structurally characterized. Recrystallization of [*t*-Bu-Pip-phos·BH_3]I from hot methanol gave colorless, block-shaped crystals. An ORTEP diagram of the structure is shown in Figure 2. The steric demand of the *tert*-butyl substituents can be seen in the bond angles shown in Table 1. The angle between the *tert*-butyl substituents has been opened up (113°) by moving one of the *tert*-butyl groups toward the less hindered face of the piperidinium substituent, which results in a relatively small C3−P−C8 angle compared to the other C−P−C angles. The C4−C3−P angle is larger than the C2−C3−P angle, showing that the piperidinium ring is skewed away from the *tert*-butyl substituents toward the BH_3. A calculated (DFT-LDA, vide infra) structure for *t*-Bu-Pip-phos shows a similar trend in bond angles. For comparison, the simplest model organic phosphine, $P(CH_3)_3$, has a calculated P−C bond distance of 1.846 Å and a C−P−C angle of 98.8°.

Catalytic Results. We have previously communicated the application of the ligands shown in Figure 1 in room-temperature Suzuki couplings of aryl bromides.[51] TPPTS gave an essentially inactive catalyst for the Suzuki coupling of 4-bromotoluene and phenylboronic acid at room temperature (Table 2). In contrast, the alkylphosphine ligands gave significantly more active catalysts under similar conditions, but with a 5-fold lower catalyst loading (0.5 vs 2.5 mol %). The *t*-Bu-Amphos and *t*-Bu-Pip-phos ligands gave complete conversion in less than 1 h, while the catalyst derived from Cy-Pip-phos gave only 46% conversion under the same conditions. In all cases, catalyst activity was

Table 2. Ligand Optimization in Aqueous-Phase Suzuki Coupling

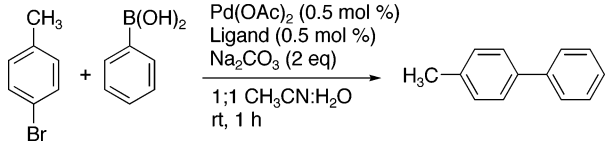

entry	ligand	L:Pd	yield (%)[a]
1	TPPTS[b]	2:1	2
2	*t*-Bu-Amphos	2:1	73
3	*t*-Bu-Amphos	1:1	98
4	*t*-Bu-Pip-phos	2:1	32
5	*t*-Bu-Pip-phos	1:1	99
6	Cy-Pip-phos	2:1	2
7	Cy-Pip-phos	1:1	46

[a] GC yield after 1 h. Mass balance was within 5%. [b] 2.5 mol % Pd, 4 h.

higher when a 1:1 L:Pd ratio was used than when a 2:1 L:Pd ratio was used. For the catalysts derived from 2:1 L:Pd ratios, *t*-Bu-Amphos gave the most active catalyst followed by *t*-Bu-Pip-phos. Cy-pip-phos gave only a trace of product under these conditions. The increased activity of the 1:1 L:Pd ratio catalyst is consistent with a monophosphine-palladium complex ("LPd(0)") being the true active species in analogy to Fu's[18] results with *t*-Bu_3P. Excellent yields were obtained with these ligands for a range of aryl bromide and arylboronic acid substrates.[51] We have applied these ligands to Heck and Sonogashira coupling reactions and see the same general trend in ligand activity.[52]

Steric and Electronic Parameters. The steric and electronic properties of *t*-Bu-Amphos, *t*-Bu-Pip-phos, and Cy-Pip-phos were determined in an effort to better understand how steric and electronic factors affect catalyst activity. The cone angle concept introduced by Tolman[53] is widely used to compare the steric demand of phosphine ligands. Tolman in the early to mid 1970s derived cone angles by examining model structures built with CPK models of ligand−Ni complexes. Since that time, advances in computers and computational methods, notably density functional theory (DFT), have enabled the calculation of geometries of molecular complexes with reasonable reliability. For example, the calculated geometry (DFT, local density approximation (LDA)) of the isolated *t*-Bu-Pip-phos ligand (Table 1) is in reasonable agreement with that of the experimental crystal structure for this phosphine complexed to BH_3. On the basis of the assumption that a single ligand complexed to palladium is the active species, we first optimized the geometries of the isolated ligand and the ligand complexed to palladium (Table 3). An interesting feature is the regularity of the Pd−P bond distance (∼2.15 Å) in the optimized structure.

We then calculated the cone angle using the approach developed by Taverner[54] and our optimized geometries for the LPd(0) complex. Taverner has developed a general approach for calculating cone angles based on solid angles, and this is incorporated in the program STERIC.[55] Using this methodology, the cone angle of *t*-Bu_3P in (*t*-Bu_3P)Pd(0) was calculated to be 190° (Table

(53) Tolman, C. A. *Chem. Rev.* **1977**, *77*, 313−348.
(54) Taverner, B. C. *J. Comput. Chem.* **1996**, *17*, 1612−1623.
(55) Taverner, B. C., *STERIC,* 1.11, http://www.ccl.net/cca/software/SOURCES/C/steric/index.shtml, 1995.

Table 3. Selected Bond Lengths (Å) and Angles (deg) for Free Ligands and LPd(0) Complexes from DFT Calculations[a]

param	*t*-Bu-Pip-phos	(*t*-Bu-Pip-phos)Pd	*t*-Bu-Amphos	(*t*-Bu-Amphos)Pd	Cy-Pip-phos	(Cy-Pip-phos)Pd	*t*-Bu_3P	(*t*-Bu_3P) Pd
P−C	1.899	1.885	1.886	1.878	1.868	1.860	1.911	1.907
P−C	1.892	1.885	1.888	1.877	1.878	1.857	1.913	1.909
P−C	1.893	1.895	1.883	1.870	1.881	1.868	1.910	1.906
P−Pd		2.153		2.150		2.144		2.161
C−P−C	110.2	109.0	111.9	112.5	105.1	105.0	106.7	108.2
C−P−C	98.6	101.2	100.7	100.7	105.3	108.3	106.7	108.2
C−P−C	111.2	108.0	100.1	103.2	96.1	100.0	106.9	108.2
Pd−P−C		111.2		114.2		114.6		110.7
Pd−P−C		114.5		112.9		116.8		110.7
Pd−P−C		112.2		112.2		110.9		110.6

[a] Determined from calculated structures (DFT, local density approximation (LDA)).

Table 4. Measured and Calculated Steric and Electronic Parameters

ligand	calc cone angle (deg)	χ (cm^{-1})[a]	q(P)[b,c] free L	HOMO[b,d] (eV) free L	GAP[b,e] (eV) free L	q(P)[b,c] LPd(0)	HOMO[b,d] (eV) LPd(0)	GAP[b,e] (eV) LPd(0)
t-Bu_3P	190	0.0	0.43	4.85	5.59	0.67	3.87	2.13
t-Bu-Amphos	194	7.5	0.46	8.23	4.44	0.61	7.22	2.37
t-Bu-Pip-phos	191	4.2	0.48	7.84	4.21	0.63	6.82	2.40
Cy-Pip-phos	186	5.8	0.45	7.98	4.11	0.69	6.71	2.46

[a] Difference in A_1 stretching frequency for $LNi(CO)_3$ from (*t*-Bu_3P)$Ni(CO)_3$. [b] Obtained at the gradient-corrected DFT level with the Becke88-Perdew86 exchange−correlation functional (B88P86). [c] Calculated charge on phosphorus atom. [d] Calculated HOMO energy level. [e] Calculated HOMO−LUMO energy gap.

4), which is larger than the 182° value determined by Tolman using CPK models for the nickel complex. The *t*-Bu-Amphos ligand was determined to have the largest cone angle (194°), while that for *t*-Bu-Pip-phos (191°) was predicted to be slightly larger than *t*-Bu_3P. Cy-Pip-phos has the least steric bulk of the ligands prepared by us, with a cone angle of 186°.

There are different ways to look at the "electronic parameters" of the ligands from experimentally derived quantities as well as those derived from computation. Tolman[53,56] has suggested that the electronic parameters of the ligands can be determined from comparing the A_1 stretching frequency of $LNi(CO)_3$ complexes to that of a standard. $LNi(CO)_3$ complexes were prepared by reacting each ligand with an excess of $Ni(CO)_4$ in CH_2Cl_2.[50,57] The electronic parameter (χ) in Table 4 is the difference between the measured stretching frequency and that of (*t*-Bu_3P)$Ni(CO)_3$. Although t-Bu-Amphos, *t*-Bu-Pip-phos, and Cy-Pip-phos are comparable in size to *t*-Bu_3P, they are less electron donating based on the higher CO stretching frequencies measured for $LNi(CO)_3$ complexes of these ligands. Of the ligands, *t*-Bu-Pip-phos (4.2 cm^{-1}) was the strongest electron donor followed by Cy-Pip-phos (5.8 cm^{-1}) and *t*-Bu-Amphos (7.5 cm^{-1}). The positively charged substituents appear to decrease the electron-donating ability of the ligands relative to structurally similar, but uncharged phosphines. For example, tricyclohexylphosphine (χ = 0.3 cm^{-1}) is a much stronger electron donor than Cy-Pip-phos (χ = 5.4 cm^{-1}) despite their similar structures. The quaternary ammonium-substituted phosphines have χ values similar to sterically undemanding alkylphosphines, such as *n*-Bu_3P, whereas they are significantly more electron donating than triphenylphosphine (χ = 12.8 cm^{-1}).[53]

We can also define electronic parameters based on computational values such as the charge on the phosphorus atom (q(P)), the highest occupied molecular orbital (HOMO) energy, and the energy difference between the HOMO and the lowest unoccupied molecular orbital (LUMO) defined as the GAP = |E(HOMO) − E(LUMO)| (Table 4). It has been shown that the GAP correlated reasonably well with the first excitation energy.[58,59] The quantities shown in Table 4 were obtained at the gradient-corrected DFT level with the Becke88-Perdew86 exchange−correlation functional (B88P86).[60,61] The charges on the phosphorus are all very similar independent of whether there is a positive charge on the ligand or not. The charges on the positively charged ligands are slightly higher than those on *t*-Bu_3P, as would be expected in both the free phosphine and the phosphine−Pd complex. The HOMO energy is lower in the complex than in the isolated ligand. The HOMO for *t*-Bu_3P is significantly lower than those of the positively charged ligands, as would be expected. This difference also carries over to the Pd−ligand complex. The GAP is substantially lowered in the complex as compared to the isolated phosphine.

Bond Dissociation Energy. Since ligand dissociation is believed to be a necessary step to form the coordinatively unsaturated active species (Scheme 1), the bond dissociation energy (BDE) for the Pd−L bond in $L_2Pd(0)$ species should correlate with catalyst activity. Gas-phase Pd−L BDE values were determined computationally at the gradient-corrected DFT level with the B88P86 functional for a range of $L_2Pd(0)$ complexes (Table 5) based on the LDA-optimized geometries. The gas-phase BDE values for the quaternary ammonium-substituted ligands were an order of magnitude lower than were determined for *t*-Bu_3P or Ph_3P. The very low BDE values for the dicationic $L_2Pd(0)$ going to the LPd(0) cation and the cationic free phosphine are due to

(56) Bartik, T.; Himmler, T. *J. Organomet. Chem.* **1985**, *293*, 343−351.
(57) Tolman, C. A. *J. Am. Chem. Soc.* **1970**, *92*, 2953−2956.
(58) Zhan, C.-G.; Nichols, J. A.; Dixon, D. A. *J. Phys. Chem. A* **2003**, *107*, 4184−4195.
(59) Garza, J.; Vargas, R.; Nichols, J. A.; Dixon, D. A. *J. Chem. Phys.* **2001**, *114*, 639−651.
(60) Perdew, J. P. *Phys. Rev. B* **1986**, *33*, 33−35.
(61) Becke, A. D. *Phys. Rev. A* **1988**, *38*, 3098−3100.

Table 5. Calculated Bond Dissociation Energies

L–Pd-L $\xrightarrow{BDE_1}$ L + L–Pd $\xrightarrow{BDE_2}$ L + Pd(0)

ligand	BDE_1[a] (kcal/mol)	BDE_2[a] (kcal/mol)
t-Bu_3P	36.0	51.5
PPh_3	34.9	49.1
t-Bu-Pip-phos	4.8	51.7
t-Bu-Amphos	5.3	52.9
Cy-Pip-phos	6.5	51.3

[a] Determined computationally at the gradient-corrected DFT level with the B88P86 functional.

charge repulsion between the two positively charged ligands in the gas phase. Counterion and solvent effects will lower this charge repulsion, leading to BDE values more similar to those observed for neutral ligands. In fact, as shown in Table 5, the ligand dissociation energies for the LPd(0) to form free phosphine and Pd are all very similar independent of the charge on the ligand. The *t*-Bu-Pip-phos ligand had the lowest dissociation energy followed by *t*-Bu-Amphos and Cy-Pip-phos, respectively, which roughly correlated with the activity of catalysts derived from these ligands.

Coordination Chemistry. Fu has shown that mixtures of *t*-Bu_3P and $Pd(dba)_2$ over a range of L:Pd ratios gave only (*t*-$Bu_3P)_2Pd(0)$.[18] This $L_2Pd(0)$ species is believed to be a resting state in the catalytic cycle, with a monophosphine species as the active catalytic species (Scheme 1). We were interested to see if the structurally similar water-soluble phosphines would behave in the same way. Dissolving a mixture of $Pd(OAc)_2$, *t*-Bu-Pip-phos (L:Pd = 2:1), sodium carbonate, and phenylboronic acid in a 1:1 mixture of acetonitrile and water gave a biphasic mixture with a brown upper organic phase and a colorless aqueous phase (eq 1). These conditions were chosen to be similar to those used in catalytic reactions, but without aryl halide. The two layers were separated and transferred to septum-sealed NMR tubes under nitrogen. Each layer was analyzed immediately by ^{31}P NMR spectroscopy. No phosphorus-containing materials were observed in the aqueous phase. The acetonitrile phase showed a single resonance at 70.4 ppm, while no free phosphine was observed (*t*-Bu-Pip-phos = 40 ppm). The observed resonance was consistent with a (*t*-Bu-Pip-phos)$_2$Pd(0) complex. In comparison, (*t*-$Bu_3P)_2Pd$ gave a resonance at 85 ppm.[18] The structure was confirmed by the ^1H and ^{13}C NMR spectra. In the ^1H NMR spectrum of the species observed at 70.4 ppm in the ^{31}P NMR, the *tert*-butyl resonance appears as an AXX′ 1:2:1 triplet (J = 6.16 Hz), rather than the doublet observed for the free ligand. The observed 1:2:1 triplet pattern is due to virtual coupling between the phosphines in a linear P–Pd–P system.[62] Similar apparent triplets were observed for each of the coupled carbons in the ^{13}C NMR spectrum of this complex.[63] This complex was not observed in the absence of phenylboronic acid (*vide infra*), so the phenylboronic acid is required to reduce the Pd(II) to Pd(0). No phosphine oxide resulting from phosphine-mediated reduction was observed, in contrast to what is commonly seen with triarylphosphines and sterically undemanding alkylphosphines.[64]

$$2\,L + Pd(OAc)_2 \xrightarrow[1{:}1\ H_2O{:}CH_3CN,\ 23\ ^\circ C]{PhB(OH)_2,\ Na_2CO_3} L\text{–}Pd\text{–}L \qquad (1)$$

L = *t*-Bu-Pip-phos, *t*-Bu-Amhos, Cy-Pip-phos

The complexation of *t*-Bu-Pip-phos and $Pd(OAc)_2$ in the presence of sodium carbonate and phenylboronic acid was repeated at L:Pd ratios of 0.5, 1, and 3. With L:Pd ratios of 0.5 and 1, the only species observed was the (*t*-Bu-Pip-phos)$_2$Pd(0) complex with a chemical shift of 70.4 ppm. At an L:Pd ratio > 2:1, the $L_2Pd(0)$ complex was observed along with free phosphine (40 ppm). Therefore, the only stable complex formed between *t*-Bu-Pip-phos and Pd(0) is the (*t*-Bu-Pip-phos)$_2$Pd(0) complex.

A similar series of complexation studies was carried out using *t*-Bu-Amphos as ligand. As with *t*-Bu-Pip-phos, all of the phosphorus-containing species partitioned into the acetonitrile phase. Using a 2:1 *t*-Bu-Amphos:Pd(OAc)$_2$ ratio, a new species with a chemical shift of 55.8 ppm was observed in the ^{31}P NMR spectrum. Apparent triplets for the *t*-Bu resonances in the ^1H NMR spectrum (J = 6.38 Hz) and all of the coupled resonances in the ^{13}C NMR spectrum confirmed a similar (*t*-Bu-Amphos)$_2$Pd(0) complex to that observed with *t*-Bu-Pip-phos. Varying the L:Pd ratio over the range of 0.5 to 3 gave only the (*t*-Bu-Amphos)$_2$Pd(0) complex and free *t*-Bu-Amphos, when the L:Pd ratio was >2.0.

The same series of studies was performed using Cy-Pip-phos as the ligand. When a 0.5:1 Cy-Pip-phos:Pd ratio was used, a major resonance was observed at 39 ppm, which has been assigned to (Cy-Pip-phos)$_2$Pd. The resonance at 39 ppm is similar to the 40 ppm resonance reported for ($Cy_3P)_2Pd$ (Cy = cyclohexyl).[65] When the L:Pd ratio was increased to 1:1, the 39 ppm resonance was still the major species, but minor resonances at 48, 43, and 26 ppm were also observed (Figure 3). In contrast to the *t*-Bu-substituted ligands, the complexation chemistry became much more complex at higher L:Pd ratios. When the L:Pd ratio was increased to 2:1, the resonance at 39 ppm was a minor peak. Major resonances were observed between 20 and 30 ppm, with additional resonances at 56, 48, and 9 (free Cy-Pip-phos) ppm. Increasing the L:Pd ratio to 3:1 resulted in a further increase in the intensity of the resonances between 20 and 30 ppm as well as the free Cy-Pip-phos resonance, while the resonance at 39 ppm had largely disappeared. Therefore, unlike the *t*-Bu-substituted ligands, the $L_2Pd(0)$ complex does not form efficiently at higher L:Pd ratios.

In an effort to simplify the reduction chemistry at high Cy-Pip-phos:Pd ratios, we chose to use sodium formate, which is known to efficiently reduce a variety of Pd(II) species, as the reductant. Dissolving a mixture of *t*-Pip-phos and $Pd(OAc)_2$ (L:Pd = 2:1) in 1:1 water/acetonitrile in the presence of an excess of sodium formate gave the expected 70 ppm resonance after <10 min. Unlike the sodium carbonate/phenylboronic acid

(62) Jenkins, J. M.; Shaw, B. L. *Proc. Chem. Soc.* **1963**, 279.
(63) See the Supporting Information for copies of the NMR spectra of this complex.
(64) Amatore, C.; Jutand, A. *J. Organomet. Chem.* **1999**, *576*, 254–278.
(65) Netherton, M. R.; Dai, C.; Neuschütz, K.; Fu, G. C. *J. Am. Chem. Soc.* **2001**, *123*, 10099–10100.

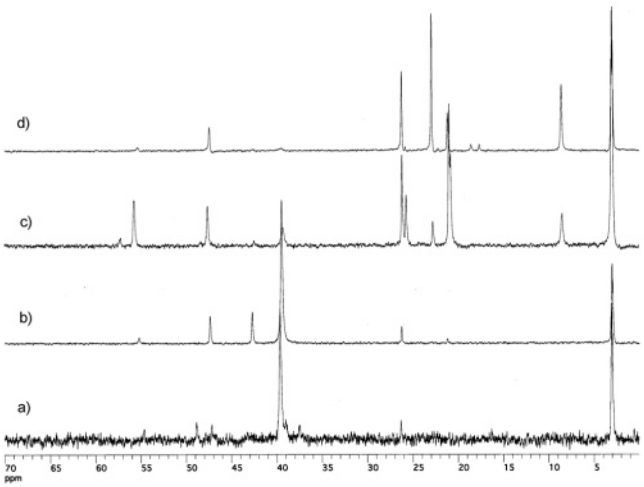

Figure 3. ^{31}P NMR spectra of Cy-Pip-phos complexation to $Pd(OAc)_2$ in the presence of phenylboronic acid and sodium carbonate after 10 min reaction time. Peak at 3 ppm is trimethyl phosphate used as an internal standard. (a) 0.5:1 Cy-Pip-phos/$Pd(OAc)_2$; (b) 1:1 Cy-Pip-phos/$Pd(OAc)_2$; (c) 2:1 Cy-Pip-phos/$Pd(OAc)_2$; (d) 3:1 Cy-Pip-phos/$Pd(OAc)_2$.

system, only a single solvent phase was obtained. Since reduction with formate occurred cleanly with the *t*-Bu-Pip-phos system, it was applied to the Cy-Pip-phos system.

A ^{31}P NMR spectrum of a mixture of Cy-Pip-phos, $Pd(OAc)_2$ (L:Pd = 1:1), and excess sodium formate in 1:1 water/acetonitrile gave a major resonance at 44 ppm and a minor resonance at 41 ppm after 10 min. After standing for 24 h, there was no change in the spectrum other than a slight increase in the relative intensity of the 41 ppm resonance. A distinct 1:2:1 triplet was observed in the ^{13}C NMR spectrum for the resonance at 33.3 ppm (J = 10.61 Hz), but the other peaks were either broadened singlets or doublets. Resonances for free acetate (181.5 and 23.6 ppm) were also observed. On the basis of the presence of the apparent triplet peak and the ^{31}P NMR chemical shift, we have assigned this structure as $(Cy\text{-}Pip\text{-}phos)_2Pd$ in analogy to the *t*-Bu-Amphos and *t*-Bu-Pip-phos complexes.

A 2:1 ratio of Cy-Pip-phos:$Pd(OAc)_2$ was reduced by an excess of sodium formate in 1:1 water/acetonitrile. The ^{31}P NMR spectrum obtained after approximately 10 min showed two resonances at 44 and 28 ppm with an integration ratio of 1:1.5. A ^{31}P NMR spectrum of the same sample after standing at room temperature for 1 h showed the same two peaks, but in a 1:0.58 ratio. Finally after standing for about 7 h, the reaction gave a single resonance at 44 ppm. Repeating the reduction with a 3:1 ratio of Cy-Pip-phos:$Pd(OAc)_2$ initially gave a more complex pattern of resonances between 25 and 28 ppm, as well as a small, broad set of peaks between 40 and 45 ppm, in the ^{31}P NMR spectrum. After standing for 24 h, the spectrum had resolved to a major peak at 28 ppm and several small resonances between 28 and 26 ppm. The $(Cy\text{-}Pip\text{-}phos)_2Pd$ resonance at 44 ppm was not observed under these conditions.

These results suggest that the 28.3 ppm resonance represents an initial species formed upon complexation of Cy-Pip-phos and $Pd(OAc)_2$. A likely candidate for the 28.3 ppm resonance would be a Pd(II) species formed upon complexation of Cy-Pip-phos, but before reduction to the Pd(0) complex. This hypothesis was confirmed by dissolving a 2:1 ratio of Cy-Pip-phos and Na_2PdCl_4 in 1:1 water/acetonitrile. A ^{31}P NMR spectrum of this mixture gave a single peak at 28.3 ppm. The ^{13}C NMR spectrum gave a pattern similar to that seen for Cy-Pip-phos with a virtual triplet at 32.2 ppm, consistent with a trans arrangement of the two phosphines in the complex. Therefore, we have assigned the 28.3 ppm resonance as arising from *trans*-$(Cy\text{-}Pip\text{-}phos)PdCl_2$. Grubbs[50] reported a chemical shift of 27.1 ppm (D_2O) for this complex prepared by an analogous procedure. The same species could be formed by reacting $Pd(OAc)_2$ with Cy-Pip-phos (L:Pd = 2:1) in the absence of reductant. Again, no phosphine-mediated reduction occurred, as judged by the fact that no phosphine oxide formed.

$$2\ \text{Cy-Pip-phos} + Na_2PdCl_4 \xrightarrow[(1:1)]{H_2O:CH_3CN} \underset{\text{L = Cy-Pip-phos}}{\overset{\text{L}}{\underset{\text{L}}{\text{Cl–Pd–Cl}}}} \qquad (2)$$

The *t*-Bu-Amphos ligand was reacted with Na_2PdCl_4 in 1:1 water/acetonitrile in an effort to prepare the *trans*-$(t\text{-Bu-Amphos})_2PdCl_2$ complex. The reaction was initially a homogeneous, golden yellow solution, but after standing for a few minutes a pale yellow precipitate formed. A ^{31}P NMR spectrum of the solution showed a pair of broad resonances at 37 and 38 ppm as well as free *t*-Bu-Amphos (22 ppm). The solid, which was sparingly soluble in acetonitrile, gave the same pair of broad resonances (38 and 40 ppm) and free *t*-Bu-Amphos, as well as some minor unidentified resonances between 60 and 65 ppm. Although the identity of this material could not be determined, it does not appear to be the *trans*-L_2PdCl_2 complex observed with Cy-Pip-phos. Due to the increased steric bulk of the *tert*-butyl-substituted ligands, it is likely that the L_2PdCl_2 structure is too sterically congested to be stable. The two peaks observed for the soluble component of the product formed from *t*-Bu-Amphos and Na_2PdCl_2 may be due to cis- and trans-isomers of $[(t\text{-Bu-Amphos})PdCl(\mu\text{-Cl})]_2$. The poor solubility of this material precluded further structural characterization.

Discussion

The *t*-Bu-Amphos and *t*-Bu-Pip-phos ligands provided highly active catalysts for Suzuki, Heck, and Sonogashira couplings, while the Cy-Pip-phos ligand gave less active catalysts.[51,52] In this work, we have attempted to address the question of why the Cy-Pip-phos ligand gave less active catalysts. This understanding would hopefully lead to more rational design of next generation ligands. The nature of steric and electronic properties of ligands on catalyst activity is often poorly understood, despite significant effort devoted to this problem over the years.

Steric and Electronic Properties. Using a combination of computational and experimental studies we have determined the steric and electronic properties of the water-soluble alkylphosphine ligands in Figure 1. The activity trend of catalysts derived from these ligands with 1:1 L:Pd ratios (*t*-Bu-Amphos ≈ *t*-Bu-Pip-

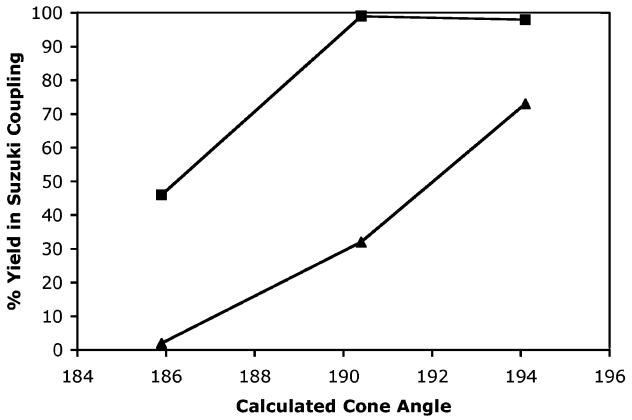

Figure 4. Correlation of calculated ligand cone angles to yields for 4-methylbiphenyl (Table 2) for 1:1 L:Pd ratios (■) and 2:1 L:Pd ratios (▲).

phos > Cy-Pip-phos)[51,52,66] increases with increasing cone angle (Figure 4). The activity of the catalyst derived from 2:1 L:Pd ratios correlates directly to the calculated cone angles for these ligands. Thus as the L:Pd ratio increases, the ability of the more sterically demanding ligands to promote ligand dissociation to give the active "LPd(0)" species becomes more important. Cone angle does not provide a full explanation for the observed catalyst activity, however. With less reactive aryl chloride substrates, *t*-Bu-Pip-phos gave a more active catalyst than *t*-Bu-Amphos despite the larger cone angle for *t*-Bu-Amphos.[51]

The electron-donating ability of the ligands determined from the Tolman χ parameter (Table 4) does not correspond with the activity of catalysts derived from these ligands. Cy-pip-phos has an intermediate χ value to those of *t*-Bu-Amphos and *t*-Bu-Pip-phos, yet gave significantly less active catalysts. Therefore, steric effects appear to be more important than the χ electronic parameter in predicting catalyst activity. The χ electronic component may account for the increased yields obtained in the Suzuki coupling of 4-chlorobenzonitrile when *t*-Bu-Pip-phos is used as the ligand compared to *t*-Bu-Amphos, however. Electron density at the metal center likely becomes more important as the aryl halide substrate becomes less reactive toward oxidative addition.

Other calculated measures of the electronic nature of the phosphine ligand (Table 4) do provide a correlation with catalytic activity. While catalyst activity shows little dependence on the charge on phosphorus in the free ligand, catalyst activity increases with decreasing positive charge on the phosphorus in the LPd(0) complex. Catalyst activity increases with increasing HOMO energy levels for the LPd(0) complex, while the HOMO energy levels of the free phosphines do not correlate well with activity. The HOMO−LUMO energy difference for both the free ligand and LPd(0) complex correlated with catalytic activity, although with opposite trends. For the free phosphine, catalyst activity increased with larger HOMO−LUMO gaps, while activity increased with decreasing GAP values for the LPd(0) complex. Further exploration of these parameters may provide new computational methods to predict catalyst activity.

(66) The relative catalytic activity of these systems has been based on product yields measured at short reaction times.

Catalyst Structure and Reactivity. The structure and reactivity of palladium complexes of the water-soluble alkylphosphine ligands have been explored through both computational and experimental methods. Computationally determined gas-phase M−L BDEs show that ligand dissociation is most difficult from (Cy-Pip-phos)$_2$Pd(0) followed by the *t*-Bu-Amphos and *t*-Bu-Pip-phos complexes, respectively (Table 4). The relatively high BDE for Cy-Pip-phos may account for its near complete lack of activity when a 2:1 L:Pd ratio is used. Although the BDE trend might be expected to correlate well with activity of catalysts derived from 2:1 L:Pd ratios, this is not the case for *t*-Bu-Amphos and *t*-Bu-Pip-phos. Clearly other factors are involved, possibly related to differences between values calculated in the gas phase, and conditions in solution.

Multinuclear NMR studies provide the most compelling difference between the properties of Cy-Pip-phos and the *tert*-butyl-substituted ligands. Both *t*-Bu-Amphos and *t*-Bu-Pip-phos rapidly form $L_2Pd(0)$ complexes in the presence of $Pd(OAc)_2$ under reducing conditions. The $L_2Pd(0)$ complex is the only phosphorus-containing species observed except at L:Pd ratios > 2:1, where free phosphine is also present. No evidence is seen for an intermediate Pd(II) complex, suggesting that the reduction occurs rapidly (<5 min). In fact, attempts to prepare *trans*-L_2PdCl_2 complexes with *t*-Bu-Amphos were unsuccessful. Instead, a poorly soluble material was formed that has tentatively been assigned as *cis*- and *trans*-[(*t*-Bu-Amphos)PdCl(μ-Cl)]$_2$. In contrast, the combination of Cy-Pip-phos and $Pd(OAc)_2$ rapidly forms $L_2Pd(0)$ only when the L:Pd ratio is ≤1, while higher Cy-Pip-phos concentrations inhibit the reduction of the intermediate palladium(II) complex. Unlike the larger *tert*-butyl-substituted ligands, Cy-Pip-phos cleanly forms an L_2PdCl_2 complex with palladium(II) precursors in the absence of reductants.

It should be noted that no evidence of phosphine-mediated reduction of palladium has been observed for these sterically demanding, electron-rich ligands. Amatore and Jutand[64] have shown that in the presence of oxygen ligands ($^-$OAc, $^-$OH, etc.), aryl and alkylphosphines will efficiently reduce palladium(II) phosphine complexes, resulting in formation of phosphine oxides. Phosphine oxide has not been observed in our ^{31}P NMR spectroscopic studies. We also do not see evidence for acetate coordination to the $L_2Pd(0)$ complexes, which Amatore and Jutand have observed. Under the biphasic conditions of the phenylboronic reaction, no acetate resonances are seen in the ^{1}H or ^{13}C NMR spectra. When formate is used as a reductant, free acetate is observed in the monophasic reaction by ^{13}C NMR spectroscopy (181.5 and 23.5 ppm) rather than palladium-bound acetate (177.2 and 21.6 ppm).

The NMR spectroscopy results show that the rate of reduction of (Cy-Pip-phos)$_2$PdCl$_2$ to (Cy-Pip-phos)$_2$Pd(0) is inversely related to the concentration of Cy-Pip-phos. Therefore, phosphine dissociation must occur as part of, or prior to, the rate-limiting step for the reduction (Scheme 2). The rate-limiting step could be the initial dissociative substitution of formate for Cy-Pip-phos (path B). Alternatively, if formate initially displaces chloride (path A), phosphine dissociation would be required for β-hydride elimination to occur.

Scheme 2. Proposed Ligand Effect on Reduction of $L_nPd(II)$ Complexes

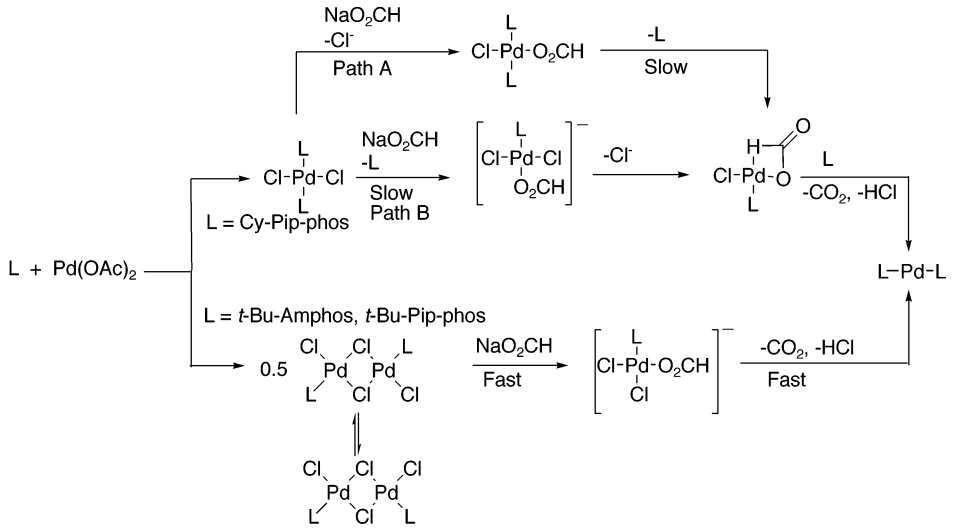

In either case, phosphine dissociation is a necessary step in the reduction mechanism. Rapid reduction of $Pd(OAc)_2$ in the presence of Cy-Pip-phos only occurs at low L:Pd ratios ($\leq$1:1). Under these conditions, not all of the $Pd(OAc)_2$ can be converted to $(Cy\text{-}Pip\text{-}phos)_2PdCl_2$. Monophosphine or uncoordinated Pd(II) species could undergo rapid reduction, since there would be less steric bulk around the metal to inhibit ligand substitution. Ligand exchange between palladium(II) and palladium(0) complexes would ultimately lead to complete reduction of the $Pd(OAc)_2$ to $(Cy\text{-}Pip\text{-}phos)_2Pd$ and phosphine-free palladium(0) species.

The *tert*-butyl-substituted ligands do not form coordinatively saturated *trans*-L_2PdCl_2 complexes, even in the absence of reductant. We have proposed that these ligands form monophosphine chloride-bridged dimers, although their low solubility precluded full characterization. The less sterically demanding monophosphine palladium dimer would be expected to undergo associative ligand substitution more readily than a highly hindered L_2PdCl_2 complex (Scheme 2). The resulting four-coordinate anionic species could dissociate an anionic ligand, allowing for fast β-hydride elimination to the $L_2Pd(0)$ complex. Since phosphine dissociation would not be needed for either step in the reduction, there should be no inhibition by excess phosphine. Over the range of L:Pd ratios studied (0.5−3:1), the reduction occurred rapidly (<5 min) in all cases.

Thus, there is an interesting size dependence upon the reduction chemistry in these systems. The very sterically demanding *tert*-butyl-substituted ligands undergo rapid reduction independent of phosphine concentration, while the smaller Cy-Pip-phos forms an L_2PdCl_2 complex whose reduction is inhibited by additional Cy-Pip-phos. The relevance of this observation to catalytic systems is not clear. The low activity of catalysts derived from 1:1 Cy-Pip-phos/$Pd(OAc)_2$ is apparently not related to slow reduction, since our results show that this system undergoes reduction at a similar rate to the *tert*-butyl-substituted ligands. The slow reduction of the 2:1 Cy-Pip-phos/$Pd(OAc)_2$ system may play a part in the inactivity of catalysts generated under these conditions, although it is likely that even when generated the $(Cy\text{-}Pip\text{-}phos)_2Pd(0)$ complex is significantly less active than its *tert*-butyl analogues. Further careful studies of reaction kinetics will allow the effect of this slow reduction on catalyst activity to be determined.

Conclusions

The combined experimental and computational results presented here suggest that the best predictor of both catalyst activity and coordination chemistry for these sterically demanding, electron-rich phosphines is the calculated cone angle. Catalyst productivity correlated closely with the calculated cone angle values. The coordination chemistry of the ligands also correlated closely to the cone angle. Ligands with calculated cone angles > 190° gave catalysts that were efficiently reduced even at high L:Pd ratios. In contrast, Cy-Pip-phos (θ = 186°) inhibited the reduction of Pd(II) at higher L:Pd ratios. While the steric parameters provide a good predictor of catalyst activity, the Tolman electronic parameter based on $LNi(CO)_3$ complexes proved to be poor predictor of catalyst activity. Other calculated measures of the electronic nature of the phosphine ligands, such as the charge on phosphorus and the HOMO energy level for the LPd(0) complex, provided better correlations to catalyst activity. Further research into the use of computationally derived steric and electronic descriptors may provide new insights into ligand design for these reactions.

Experimental Section

General Procedures. The syntheses of *t*-Bu-Pip-phos,[51] *t*-Bu-Amphos,[51] and Cy-Pip-phos[50] have been previously reported. All other reagents were obtained from commercial sources and used without further purification. Aqueous solvent mixtures of acetonitrile were sparged with nitrogen for 15 min prior to use. ^{31}P NMR spectra were obtained on a Bruker-Aspect 500 MHz instrument at 202.5 MHz and were externally referenced to 85% H_3PO_4 in D_2O (0.0 ppm) or internally referenced to trimethyl phosphate (3.0 ppm). ^1H and ^{13}C NMR spectra were obtained on a Bruker Aspect 360 MHz instrument and were referenced to solvent resonances.

Structural Characterization. A suitable crystal for X-ray characterization was mounted on a glass fiber and transferred to the goniometer. The crystal was cooled to −100 °C in a

stream of nitrogen gas, and the data were collected on a Brüker SMART diffractometer with a CCD area detector, using graphite-monochromated Mo Kα radiation. SHELXTL software, version 6.14, was used for solution and refinement.[67] Absorption corrections were made with SADABS.[68] The structure was refined by full-matrix least-squares on F^2.

Computational Details. We have previously shown that the geometries and frequencies of transition metal complexes[69−72] can be predicted reliably at the local density functional theory level.[73] Geometries were optimized at the local DFT level with the DZVP basis set[74] where the heavy atoms are polarized double-ζ and the hydrogen atoms have a double-ζ basis set. Because Pd is a second-row transition metal, we need to consider the effects of relativity. To minimize these effects, we have used the Stuttgart relativistic pseudopotential and the associated basis set.[75] There are 28 electrons in the core of the ECP, and the basis set for Pd is contracted to [6s5p3d]. The basis set for the auxiliary fitting basis set was taken from the work of Chen[76] as incorporated into the DGauss program system. The calculations at the local level were done with the potential fit of Vosko, Wilk, and Nusair for the exchange−correlation functional.[77] Geometries were optimized by using analytic gradients. Due to the size of the molecules, vibrational frequencies were not calculated. The calculations were done with the program DGauss on Silicon Graphics computers.[78−80] The atomic charges, orbital energies, and dissociation energies were calculated at the gradient-corrected level with the B88P86 exchange−correlation functional, the DZVP basis set, and the LDA optimized geometries. The cone angles were calculated form the LDA optimized geometries for the monomer−Pd complex by using the STERIC[54,55] program and the volumetric parameters therein with the Pd atom set at the origin.

General Procedure for Measurement of χ Electronic Parameter. Solutions of $LNi(CO)_3$ complexes were prepared according to the procedure reported by Grubbs.[50] Thus, the phosphine (0.18 mmol) was dissolved in 3 mL of CH_2Cl_2 in a drybox under nitrogen. $Ni(CO)_4$ (20 μL, 0.18 mmol, CAUTION, highly toxic, volatile liquid) was added to the solution, and the mixture was sealed and allowed to stir for 15 min. At this time, 100 μL of the reaction mixture was diluted to 1 mL with CH_2Cl_2. The IR spectra were obtained in an air-free solution cell (NaCl windows). (*t*-Bu-Pip-phos)$Ni(CO)_3$: 2060.3 cm^{-1}. (*t*-Bu-Amphos)$Ni(CO)_3$: 2063.6 cm^{-1}. (Cy-Pip-phos)$Ni(CO)_3$: 2061.9 cm^{-1}.

General Procedure for Generation of $L_2Pd(0)$ in the Presence of Phenylboronic Acid. In a drybox, $Pd(OAc)_2$ (0.035 mmol), ligand (0.5−3 equiv relative to Pd), Na_2CO_3 (0.67 mmol), and phenylboronic acid (0.29 mmol) were added to a screw-cap vial sealed with a septum. A degassed solution of acetonitrile/water (1:1, 1 mL) was added via syringe under nitrogen purge. The reaction was allowed to stir at room temperature for 5 min. After 5 min, formation of a biphasic solution was observed, and each layer was taken up by syringe and added to a septum-sealed NMR tube under nitrogen and analyzed by ^{31}P NMR spectroscopy. Samples prepared from 2:1 ratios of *t*-Bu-Pip-phos or *t*-Bu-Amphos to $Pd(OAc)_2$ were also characterized by ^1H and ^{13}C NMR spectroscopy.

(*t*-Bu-Pip-phos)$_2$Pd(0). An NMR sample was prepared as described above for a 2:1 ratio of *t*-Bu-Pip-phos/$Pd(OAc)_2$. The aqueous phase showed no resonances in the ^{31}P NMR spectrum and was not further analyzed. Acetonitrile layer: ^1H NMR (CD_3CN/D_2O, 360 MHz): δ 3.28 (brd, J = 11.72 Hz, 2H), 3.09 (brt, J = 12.96 Hz, 2H), 2.95 (s, 3H), 2.84 (s, 3H), 2.50 (brd, J = 12.33 Hz, 2.09 (brq, J = 13.55 Hz, 2H), 1.82 (brm, 1H), 1.32 (virtual triplet (vt,), J_{H-P} = 6.16 Hz, 18H). ^{13}C NMR (CD_3CN/D_2O, 90.6 MHz): δ 64.1 (vt, J_{C-P} = 5.31 Hz), 56.9, 47.8, 36.2 (vt, J_{C-P} = 2.65 Hz), 33.0, 31.7 (vt, J_{C-P} = 6.63, 5.31 Hz), 28.3 (vt, J_{C-P} = 5.31 Hz). ^{31}P NMR (CD_3CN/D_2O, 202.5 MHz): δ 70.4 (s).

(*t*-Bu-Amphos)$_2$Pd(0). An NMR sample was prepared as described above for a 2:1 ratio of *t*-Bu-Amphos/$Pd(OAc)_2$. The aqueous phase showed no resonances by ^{31}P NMR spectroscopy and was not further analyzed. Acetonitrile layer: ^1H NMR (CD_3CN/D_2O, 360 MHz): δ 3.64 (brm, 2H), 2.98 (s, 9H), 1.75 (brm, 2H), 1.26 (vt, J_{H-P} = 6.38 Hz, 18H). ^{13}C NMR (CD_3CN/D_2O, 90.6 MHz): δ 69.9 (vt, J = 17.65, 18.03 Hz), 53.5 (t (1:1:1), J_{C-N} = 4.16 Hz), 35.5 (vt, J = 5.55 Hz), 30.6 (vt, J = 5.55 Hz), 16.7. ^{31}P NMR (CD_3CN/D_2O, 202,5 MHz): δ 55.8 (s).

(Cy-Pip-phos)$_2$Pd(0). An NMR sample was prepared as described above for a 1:1 ratio Cy-Pip-phos/$Pd(OAc)_2$. Acetonitrile layer: ^{31}P NMR (CD_3CN/D_2O, 202.5 MHz): δ 55.0 (s, integral = 0.07), 47.4 (s, integral = 0.11), 42.6 (s, integral = 0.17), 39.6 ppm (s, integral = 1.0), 26.3 (s, integral = 0.06), 21.2 (s, integral = 0.02).

General Procedure for Preparation of $L_2Pd(0)$ in the Presence of Sodium Formate. In the drybox, a vial was charged with $Pd(OAc)_2$ (0.035 mmol), ligand (0.5−3 equiv to Pd), and sodium formate (0.7 mmol). A degassed solution of acetonitrile/water (1:1, 1 mL) was added by syringe to the sealed vial containing the solid reagents. The reaction was allowed to stir at room temperature for 5 min, at which point the solution was transferred to a septum-sealed NMR tube by syringe and analyzed by ^{31}P NMR spectroscopy. The sample produced from a 1:1 ratio of Cy-pip-phos/$Pd(OAc)_2$ was also analyzed by ^1H and ^{13}C NMR spectroscopy.

(*t*-Bu-Pip-phos)$_2$Pd(0). An NMR sample was prepared as described above with a 1:1 ratio of *t*-Bu-Pip-phos/$Pd(OAc)_2$. ^{31}P NMR (CH_3CN/H_2O, 202.5 MHz): δ 70 (s).

(Cy-Pip-phos)$_2$Pd(0). A 1:1 mixture of Cy-Pip-phos/$Pd(OAc)_2$ was reduced by sodium formate as described above. ^{13}C NMR (CD_3CN/D_2O, 90.6 MHz): δ 63.4, 57.1, 47.8, 33.3 (vt, J_{C-P} = 10.61 Hz), 30.5, 30.2, 27.9 (d, J_{C-P} = 14.6 Hz), 26.7, 24.3. A second minor set of resonances with similar pattern was also observed.[63] Free acetate was also observed at 181.5 and 23.6 ppm. ^{13}P NMR (CD_3CN/D_2O, 202.5 MHz): δ 44 (s), 41 (s, minor).

Complexation of *t*-Bu-Amphos with $Pd(OAc)_2$. In the drybox, $Pd(OAc)_2$ (9.0 mg, 0.04 mmol) and *t*-Bu-Amphos (20.7 mg, 0.08 mmol) were added to a screw-cap vial, which was sealed with a septum and dissolved in degassed D_2O. The reaction was allowed to stir at room temperature for 5 min, during which time a pale yellow precipitate formed. The D_2O solution showed resonances for *t*-Bu-Pip-phos and two new species at 37 and 38 ppm in the ^{31}P NMR spectrum. The solid precipitate was sparingly soluble in acetonitrile. A ^{31}P NMR

(67) Sheldrick, G. M. *SHELXTL,* Version 6.14; Brüker Advanced X-Ray Solutions, Inc., 2000.
(68) Sheldrick, G. M. Program for Semiempirical Absorption Correlation of Area Detector Data; University of Göttingen: Germany, 1996.
(69) Sosa, C.; Andzelm, J.; Elkin, B. C.; Wimmer, E.; Dobbs, K. D.; Dixon, D. A. *J. Phys. Chem.* **1992**, *96*, 6630−6636.
(70) Christe, K. O.; Dixon, D. A.; Mack, H. G.; Oberhammer, H.; Pagelot, A.; Sanders, J. C. P.; Schrobilgen, G. J. *J. Am. Chem. Soc.* **1993**, *115*, 11279−11284.
(71) Casteel, W. J., Jr.; Dixon, D. A.; Mercier, H. P. A.; Schrobilgen, G. J. *Inorg. Chem.* **1996**, *35*, 4310−4322.
(72) Casteel, W. J., Jr.; Dixon, D. A.; LeBlond, N.; Mercier, H. P. A.; Schrobilgen, G. J. *Inorg. Chem.* **1998**, *37*, 340−353.
(73) Parr, R. G.; Yang, W. *Density-Functional Theory of Atoms and Molecules*; Oxford University Press: New York, 1989.
(74) Godbout, N.; Salahub, D. R.; Andzelm, J.; Wimmer, E. *Can. J. Chem.* **1992**, *70*, 560−571.
(75) Küchle, W.; Dolg, M.; Stoll, H.; Preuss, H. *J. Chem. Phys.* **1994**, *100*, 7535−7542, and references therein; http://www.theochem.uni-stuttgart.de/pseudopotentials/.
(76) Chen, H.; Krasowski, M.; Fitzgerald, G. *J. Chem. Phys.* **1993**, *98*, 8710−8717.
(77) Vosko, S. J.; Wilk, L.; Nusair, W. *Can. J. Phys.* **1980**, *58*, 1200.
(78) Andzelm, J.; Wimmer, E.; Salahub, D. R. In *The Challenge of d and f Electrons: Theory and Computation*; Salahub, D. R., Zerner, M. C., Eds.; ACS Symposium Series, No. 394, American Chemical Society: Washington, D.C., 1989; p 228.
(79) Andzelm, J. In *Density Functional Theory in Chemistry*; Labanowski, J., Andzelm, J., Eds., Springer-Verlag: New York, 1991; p 155.
(80) Andzelm, J.; Wimmer, E. *J. Chem. Phys.* **1992**, *96*, 1280−1303.

spectrum of this mixture showed free *t*-Bu-Amphos and a pair of resonances at 38 and 40 ppm.

***trans*-(Cy-Pip-phos)$_2$PdCl$_2$.** In the drybox, Na_2PdCl_4 (3.0 mg, 0.020 mmol) and Cy-Pip-phos (13.8 mg, 0.040 mmol) were added to a screw-cap vial, which was sealed with a septum. A degassed solution of acetonitrile/water (1:1, 1 mL) was added by syringe under nitrogen. The reaction was allowed to stir at room temperature for 5 min and then analyzed by ^{31}P, ^{1}H, and ^{13}C NMR spectroscopy. ^{1}H NMR (CD_3CN/D_2O, 360 MHz): δ 3.42 (d, J = 12.76 Hz, 2H), 3.19 (brt, J = 6.76, 6.11 Hz, 2H), 3.05 (s, 3H), 3.02 (s, 3H), 2.39−2.58 (m, 4H), 1.90−2.05 (m, overlapped with solvent peak), 1.58−1.76 (m, 10H), 1.18−1.29 (m, 6H). ^{13}C NMR (CD_3CN/D_2O, 90.6 MHz): δ 62.6, 56.3, 47.1 32.5 (vt, J_{C-P} = 9.71 Hz), 29.7, 29.4, 27.1 (d, J_{C-P} = 9.71 Hz), 26.0, 22.9. ^{31}P NMR (CD_3CN/D_2O, 202.5 MHz): δ 28.3 (s).

Acknowledgment. The National Science Foundation (CHE-0124255) and The University of Alabama School of Mines and Energy Development (SOMED), the Chemical Sciences, Geosciences and Biosciences Division, Office of Basic Energy Sciences, U.S. Department of Energy (DOE) (catalysis center program), and the Robert Ramsay Chair Foundation provided financial support of this work. The computational work was performed, in part, by using facilities in the W. R. Wiley Environmental Molecular Sciences Laboratory, a national scientific user facility sponsored by DOE's Office of Biological and Environmental Research and located at Pacific Northwest National Laboratory, operated for DOE by Battelle. Dr. Ken Belmore and Prof. Russell Timkovich are acknowledged for their help with the NMR studies reported herein. R.B.D. thanks The University of Alabama Alumni Association and the DOE for fellowships.

Supporting Information Available: Experimental details and characterization data for *t*-Bu-Pip-phos, *t*-Bu-Amphos, and Cy-Pip-phos and complexes of these ligands; crystallographic data for [*t*-Bu-Pip-phos·BH_3]I; calculated optimized molecular geometries; and NMR spectra of ligands and coordination compounds. This material is available free of charge via the Internet at http://pubs.acs.org.

OM049241W